

Two-path interference in the resonance-enhanced few-photon ionization of atoms

B.P. Acharya,¹ S. Dubey,¹ K.L. Romans,¹ A.H.N.C. De Silva,¹
K. Foster,¹ O. Russ,¹ K. Bartschat,² N. Douguet,³ and D. Fischer¹

¹*Physics Department and LAMOR, Missouri University of Science & Technology, Rolla, MO 65409, USA*

²*Department of Physics and Astronomy, Drake University, Des Moines, Iowa 50311, USA*

³*Department of Physics, Kennesaw State University, Kennesaw, Georgia 30144, USA*

(Dated: April 27, 2022)

We investigate the resonance-enhanced few-photon ionization of atomic lithium by linearly polarized light whose frequency is tuned near the $2s - 2p$ transition. Considering the direction of light polarization orthogonal to the quantization axis, the process can be viewed as an atomic “double-slit experiment” where the $2p$ states with magnetic quantum numbers $m_\ell = \pm 1$ act as the slits. In our experiment, we can virtually close one of the two slits by preparing lithium in one of the two circularly polarized $2p$ states before subjecting it to the ionizing radiation, thereby allowing us to extract interference term between the two pathways and obtain complex phase information on the final state. The analysis of our experimental results is supported by numerical calculations.

I. INTRODUCTION

Two-path interference is one of the most intriguing and intensely studied phenomena in physics. It was first demonstrated in 1801 for optical light by Thomas Young in his well-known double-slit experiment [1]. The historic importance of this experiment for the development of quantum theory is hard to overstate, because it reveals the wave nature of massive particles such as electrons [2, 3], atoms [4], and even large molecules [5], thereby supporting de Broglie’s hypothesis of wave-particle duality [6]. Until today, this phenomenon has not lost its appeal, and it has been observed in numerous systems. On one hand, it allows to extract phase information on wave functions, which is commonly not directly observable. On the other hand, it is exploited in many quantum-control schemes, because the manipulation of the relative amplitudes of the two pathways makes it possible to control the final state with high sensitivity. In atomic and molecular scattering processes, examples include well-known effects like Feshbach, shape, and Fano resonances (e.g. [7–10]), or atomic-scale double-slits formed by diatomic molecules exhibiting interferences in differential ionization cross sections due to ion [11–14], electron [15, 16], or photon impact [17, 18].

Multiphoton ionization processes of single atoms expose two- and multi-path interferences in a particularly clean way, because of the well-defined energy and limited angular momentum transfer in photon absorption reactions. A prominent example is RABBITT (Reconstruction of Attosecond Beating by interference of Two-Photon Transitions) spectroscopy [19–22], which has become the standard tool to characterize extreme-ultraviolet (XUV) attosecond pulse trains and allows the study of attosecond atomic dynamics in the time domain. Two-color ionization schemes using (lower) harmonic radiation [23–26] enable the coherent control of the reactions’ final state via two-path interferences. Recently, other schemes have been considered, where double-slit structures in so-called Kramers-Henneberg states emerge

through the distortion of a bound state by an external field, once again resulting in interference patterns [27]. Two-path interference has not only been observed in laser pulses but also using two mutually incoherent (i.e., without mutual phase lock) continuous-wave (cw) lasers in the two-photon ionization of rubidium atoms [28], where the photon energies are tuned to two different resonances.

In the present study, two-path interference occurs in the ground-state ionization of lithium exposed to single-color femtosecond laser pulses, which are linearly polarized in the y direction. The laser spectrum has its center wavelength at 660 nm and partially overlaps with the $2s - 2p$ resonance at 671 nm. For the quantization axis chosen as the z direction, the absorption of a single photon results in the excitation to the $2p$ state coherently populating the two magnetic sublevels with $m_\ell = +1$ and -1 , respectively. These two eigenstates resemble the two “slits” in analogy to Young’s double-slit scheme (see Fig. 1). From these two excited levels, the atom is ionized without further resonance-enhancement by the absorption of two more photons from the same laser pulse. The final result is a superposition of electronic p and f continuum waves.

It is important to note that the distinction of these two pathways relies on the choice of the quantization direction. However, this choice is motivated by the experimental capability of preparing the atoms selectively in one of the two excited and polarized magnetic sublevels of the $2p$ state before exposing them to the femtosecond laser pulse. This enables us to measure not only the final intensity of the two interfering pathways, which corresponds to the differential cross sections for the ionization of the $2s$ state, but also the intensity of each pathway individually via $2p$ ionization. This fact can approximately be expressed as

$$|\mathcal{A}_{2s}(\mathbf{p})|^2 \approx \alpha |\mathcal{A}_{2p}^+(\mathbf{p}) + \mathcal{A}_{2p}^-(\mathbf{p})|^2 \quad (1)$$

where $\mathcal{A}_{2s}(\mathbf{p})$, $\mathcal{A}_{2p}^+(\mathbf{p})$, and $\mathcal{A}_{2p}^-(\mathbf{p})$ represent the ionization amplitudes for a photoelectron with asymptotic momentum \mathbf{p} from the initial $2s$ ($m_\ell = 0$), $2p$ ($m_\ell = +1$),

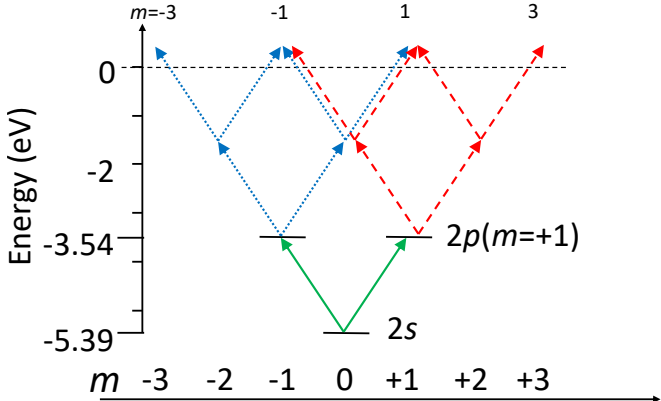


FIG. 1. Few-photon ionization scheme in lowest-order perturbation theory. The ionization pathways from the $2p$ state with $m_\ell = +1$ and -1 are shown as red dashed and blue dotted arrows, respectively. The $2s$ ionization corresponds to the superposition of both.

and $2p$ ($m_\ell = -1$) states, respectively, while α is a real factor. Equation (1) holds in our case as it follows the assumptions that (i) the light frequency is tuned near the $2s - 2p$ transition such that only resonant transitions to the $2p$ states through the first photon absorption contribute (virtual excitations can be neglected), and (ii) the field is sufficiently weak that the $2p$ state gets populated adiabatically (no Rabi oscillations between $2s$ and $2p$ states). In addition, the experimental observations and calculations will be shown to be in excellent agreement, thereby providing another evidence of the validity of Eq. (1). Using this approach, we obtain a direct and intuitive way to extract the complex phase difference between \mathcal{A}_{2p}^+ and \mathcal{A}_{2p}^- as a function of the electron emission angle, thereby revealing the effect of the orientation of the initial electron orbital angular momentum on the final state's phase.

II. METHODS

The experimental technique and the theoretical method are identical to those reported in previous studies on very similar systems [29–31]. Therefore, only some key features are repeated here and parameters specific to the present study are mentioned.

Lithium atoms are cooled and confined in a volume of about 1 mm diameter in a near-resonant all-optical atom trap (AOT) [32] with a fraction of about 25 % being in the polarized excited $2p$ ($m_\ell = +1$) state and about 75 % in the $2s$ ground state. The atoms are ionized in the field of a femtosecond laser based on a Ti:Sa oscillator with two noncollinear optical parametric amplifier (NOPA) stages. For the present study, the laser wavelength was chosen to center at 660 nm with pulse durations (FWHM of intensity) of about 65 fs and a peak intensity of about 3×10^{10} W/cm². The three-dimensional

electron momentum vectors are measured with a resolution of about 0.01 a.u. [33] in a reaction microscope (e.g., [34, 35]). It is important to note that this experimental setup enables us to obtain differential cross-normalized data for the ionization of the $2s$ and the $2p$ initial states simultaneously.

In our theoretical model, the lithium atoms are approximated as a single active electron moving in the field of a $1s^2$ ionic core. The latter is described by a static Hartree potential [36, 37], which is supplemented by phenomenological terms to account for the core polarizability as well as exchange between the valence electron and those in the core [29]. The (complex) final-state wave function is obtained after propagating the initial state in time by numerically solving the time-dependent Schrödinger equation (TDSE).

III. RESULTS AND DISCUSSION

In the present study, lithium atoms in the $2s$ ground state and $2p$ excited state are ionized in a laser field with a central wavelength of 660 nm at intensities well below 10^{11} W/cm². This situation corresponds to Keldysh parameters $\gamma > 20$, and hence the system is expected to be well described in a multi-photon picture. The two initial states are ionized by the absorption of (at least) three or two photons, respectively, resulting in a final electron energy of about 200 meV. The measured and calculated electron momentum spectra shown in Fig. 2 are in excellent agreement with each other. Before proceeding to the analysis of the two-path interference introduced above, two important features of the data should be mentioned, even though they were already reported previously in several recent studies [29, 31].

First, while the photoelectron momentum distributions (PMDs) for $2s$ ionization exhibit reflection symmetry with respect to the laser electric field direction (the vertical direction in the momentum spectra shown in Fig. 2), this symmetry is broken for ionization of the polarized $2p$ state. Consequently, the main electron emission direction appears to be shifted. The dependence of this phenomenon, known as magnetic dichroism, on the laser wavelength and intensity was recently investigated by Acharya *et al.* [31]. In this earlier study, these asymmetries were explained in a partial-wave picture. They were traced back to a nonvanishing mean orientation of the final electron orbital angular momentum $\langle m_\ell \rangle \neq 0$. This “remnant” of the initial target polarization is partially preserved throughout the ionization process. The angular shifts and observed asymmetries are then a result of the interference between (phase-shifted) partial waves with different m_ℓ .

Second, the azimuthal photoelectron angular distributions (PADs) for $2p$ ionization feature six peaks. As discussed below, this indicates beyond lowest-order contributions to the ionization cross section. Generally, the dependence of the differential cross sections on the

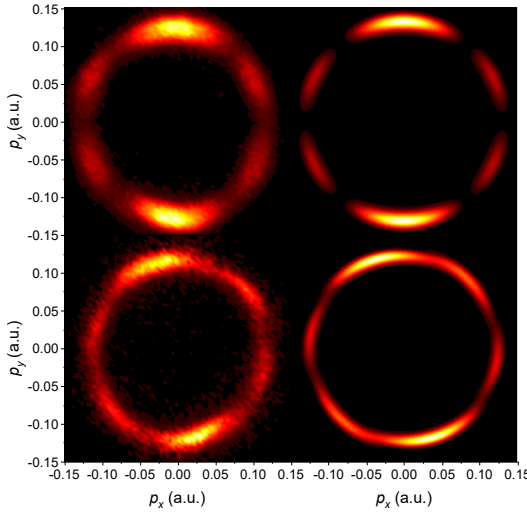


FIG. 2. Experimental (left) and theoretical (right) PMDs projected onto the xy plane for few-photon ionization of the $2s$ (top row) and $2p$ ($m_\ell = +1$) (middle row) initial states by linearly polarized laser pulses of 65 fs duration with a center wavelength of 660 nm and a peak intensity of 3.1×10^{10} W/cm 2 . The laser polarization direction is along the y axis (i.e., vertical), while the atomic initial orbital angular momentum is oriented in the z direction (i.e., perpendicular to the drawing plane).

azimuthal angle φ is given by [31]

$$\frac{d\sigma}{d\Omega} = \left| \sum_{m_\ell} c_{m_\ell} e^{im_\ell \varphi} \right|^2, \quad (2)$$

where the factors c_{m_ℓ} relate to the complex amplitudes of the partial waves. In lowest-order perturbation theory (LOPT), the absorption of only the minimum number of photons is considered. For the present initial $2p$ ($m_\ell = +1$) state, this corresponds to two-photon absorption. In the electric dipole approximation, this results in partial waves with $m_\ell = -1, +1$, and $+3$ contributing to the final state (cf. Fig. 1). For this set of dipole-allowed m_ℓ values, therefore, the above expression results in a photoelectron angular distribution with no more than four peaks, in contrast to the six peaks observed in both the experiment and the *ab initio* calculation. This evident violation of LOPT close to the $2s - 2p$ resonance was reported and discussed in our previous study as well: It is explained by the coupling between the $2s$ and $2p$ states in the external field giving rise to adiabatic population transfer between these two states and resulting in a contribution of $m_\ell = -3$ to the final state. Accounting for this additional pathway, the expression in Eq. (2) allows for angular distributions with up to six peaks, which is consistent with experiment and calculation.

The validity of the two-path interference expression given in Eq. (1) can be tested by using our theoretical description. In a first step, the \mathcal{A}_{2p}^- and \mathcal{A}_{2p}^+ amplitudes for

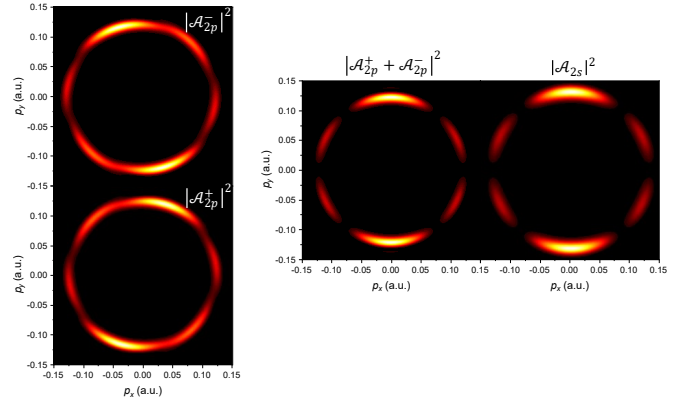


FIG. 3. Absolute square of the calculated wave functions \mathcal{A}_{2p}^+ and \mathcal{A}_{2p}^- (left), of their coherent sum $\mathcal{A}_{2p}^+ + \mathcal{A}_{2p}^-$ (center), and of \mathcal{A}_{2s} (right) in the xy plane in momentum space. See text for details.

the ionization of the $2p$ initial states with $m_\ell = -1$ and $+1$, respectively, are calculated. Their absolute squares, corresponding to the differential ionization cross sections, are shown as a function of the photoelectron momentum in Fig. 3 (left) considering only electron emission in the xy plane (i.e., for a polar angle $\vartheta = 90^\circ$). Due to symmetry considerations, the systems with opposite initial orbital angular momentum $m_\ell = +1$ and -1 are mirror images of one another with the mirror plane spanned by the laser polarization direction (the y axis) and the direction of the initial atomic polarization (the z axis). Specifically, $\mathcal{A}_{2p}^+(\sigma_{yz}\mathbf{p}) = \mathcal{A}_{2p}^-(\mathbf{p})$, where σ_{yz} is the reflection operator through the yz plane.

In the second step, Eq. (1) is tested by comparing the calculated momentum distribution for $2s$ ionization (corresponding to $|\mathcal{A}_{2s}|^2$) with the intensity of the superposition of the two amplitudes for $2p$ ionization $|\mathcal{A}_{2p}^+ + \mathcal{A}_{2p}^-|^2$. The PMDs obtained by both methods are shown in Fig. 3 (right and center, respectively). They are in overall very good agreement indeed, although the $|\mathcal{A}_{2s}|^2$ distribution has a slightly larger diameter. This small discrepancy is a result of slightly different (by approximately 10 %) photoelectron energies for $2s$ and $2p$ ionization, because the wavelength of the ionizing field is off the $2s - 2p$ resonance by about 10 nm.

The discussion above shows that the final momentum distribution for $2s$ ionization (which corresponds to $|\mathcal{A}_{2s}|^2$) can be calculated, to a good approximation, from the \mathcal{A}_{2p}^+ ionization amplitude by exploiting Eq. (1) and the mirror symmetry between \mathcal{A}_{2p}^+ and \mathcal{A}_{2p}^- . Evidently, this is not possible with the experimental data because only the absolute square of the final-state wave function $|\mathcal{A}_{2p}^+|^2$ is directly measured. However, the relative phase between \mathcal{A}_{2p}^- and \mathcal{A}_{2p}^+ can be extracted from Eq. (1) by reversing the above procedure and solving for the phase

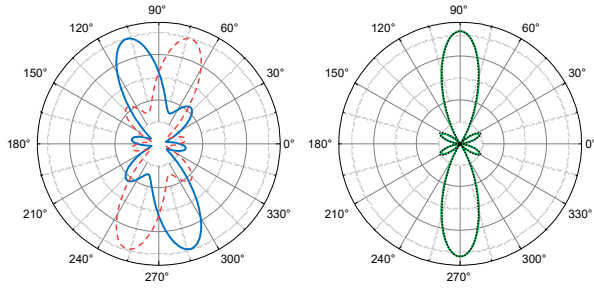


FIG. 4. Angular distributions extracted from the wave functions in Fig. 3 as a function of the photoelectron azimuthal angle φ . Left: angular distribution of $|\mathcal{A}_{2p}^+|^2$ (solid blue line) and $|\mathcal{A}_{2p}^-|^2$ (dashed red line). Right: $|\mathcal{A}_{2p}^+ + \mathcal{A}_{2p}^-|^2$ (dashed black) and $|\mathcal{A}_{2s}|^2$ (solid green).

difference. This yields

$$\cos \Delta\phi(\mathbf{p}) = \frac{|\mathcal{A}_{2s}(\mathbf{p})|^2 - \alpha |\mathcal{A}_{2p}^+(\mathbf{p})|^2 - \alpha |\mathcal{A}_{2p}^-(\mathbf{p})|^2}{2\alpha |\mathcal{A}_{2p}^+(\mathbf{p})| |\mathcal{A}_{2p}^-(\mathbf{p})|} \quad (3)$$

where $\Delta\phi(\mathbf{p}) = \arg[\mathcal{A}_{2p}^{+*}(\mathbf{p})\mathcal{A}_{2p}^-(\mathbf{p})]$. The reconstruction of the phase difference $\Delta\phi$ in three-dimensional momentum space from experimental data using Eq. (3) requires matching photoelectron energies for $2s$ and $2p$ ionization, which is not strictly fulfilled for the present laser wavelength. The question arises whether, in spite of the small photoelectron energy mismatch, Eq. (3) is still applicable if only the dependence on the electron emission angle is considered (i.e., for the electron energy fixed at the peak energy). This can be the case, if the angular distributions do not significantly vary with small shifts of the photoelectron energy. This is tested by comparing the calculated angular distributions for $2s$ ionization (extracted from $|\mathcal{A}_{2s}|^2$) with the distribution obtained for the interfering wave functions $|\mathcal{A}_{2p}^+ + \mathcal{A}_{2p}^-|^2$. The corresponding angular distributions are shown in Fig. 4. Indeed, the angular spectrum obtained from the interfering wave functions closely resembles the distribution calculated for $2s$ ionization. There is only a small deviation in the relative intensity of the main peak in the polarization direction and the side peaks. Therefore, we conclude that Eq. (3) makes it possible to extract the phase difference $\Delta\phi$ (to a good approximation) as a function of the azimuthal angle for the peak photoelectron energy.

Before Eq. (3) can be employed to calculate the phase difference $\Delta\phi$ from the experimental data, the factor α must be determined. Here we can borrow an idea from Young's double-slit experiment, where we know that the total flux is conserved, i.e., the total intensity equals the sum of the intensities going through each slit individually. In our case, this means that the momentum-integrated interference term in Eq. (1) should vanish

$$\int d^3p |\mathcal{A}_{2p}^+(\mathbf{p})| |\mathcal{A}_{2p}^-(\mathbf{p})| \cos[\Delta\phi(\mathbf{p})] = 0. \quad (4)$$

Equation (4) holds since the azimuthal dependence of the

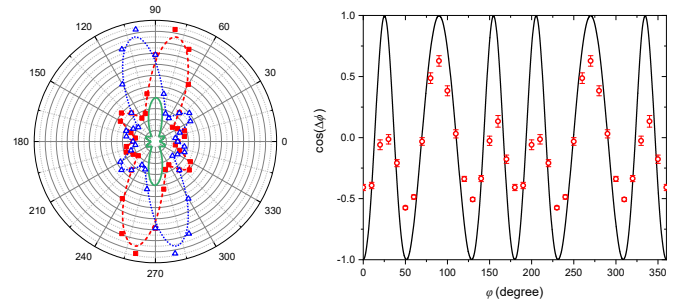


FIG. 5. Left: Experimental PADs as a function of the azimuthal angle φ for the few-photon ionization of lithium initially in the $2s$ (solid green line) and $2p$ state with $m_\ell = +1$ (red dashed line and solid squares) and -1 (blue dotted line and open triangles). The lines are interpolating splines to guide the eye. Right: Experimental and theoretical cosine of the phase difference as a function of the photoelectron azimuthal angle φ .

interference is expressed as the superposition of terms of the form $|c_n||c_m| \cos[(n-m)\phi]$, where $n \neq m$, and in this case $\int_0^{2\pi} d\phi \cos[(n-m)\phi] = 0$. Therefore, the interference term does not contribute to the total intensity, and the factor α is readily found as

$$\alpha = \frac{\int d^3p |\mathcal{A}_{2p}^+(\mathbf{p})|^2 + \int d^3p |\mathcal{A}_{2p}^-(\mathbf{p})|^2}{\int d^3p |\mathcal{A}_{2s}(\mathbf{p})|^2}. \quad (5)$$

The experimental PADs are shown in Fig. 5 (left). While the distributions for the ionization for the $2s$ and the $2p$ ($m_\ell = +1$) initial states are measured directly in our experiment, the data for $2p$ ($m_\ell = -1$) are obtained by reflecting the data for the opposite target polarization on the laser polarization axis. Using these angular distributions, the cosine of the phase difference is calculated with Eq. (3), plotted in Fig. 5 (right), and compared to the theoretical predictions.

The distribution features six crests and troughs whose positions agree very well between theory and experiment. However, some discrepancies in the magnitude persist. While the calculated curve reaches the maximum and minimum values of $+1$ and -1 , respectively, the oscillation is weaker in the experimental data. Generally, a value of $+1$ for $\cos \Delta\phi$ corresponds to maximum constructive interference, which is expected at angles where the angular distribution for $2s$ ionization has a local maximum. Correspondingly, $\cos \Delta\phi = -1$ means complete destructive interference, which should occur at local minima in the differential $2s$ ionization data.

There are two effects that might blur these interferences in the experimental data: (1) There is a small, but nonnegligible experimental angular uncertainty. (2) The experimental data represent an average over a laser intensity range, as already discussed above. As the angular distributions are not entirely independent of the laser intensity (see Fig. 2), this will also result in a blurring of the angular distribution.

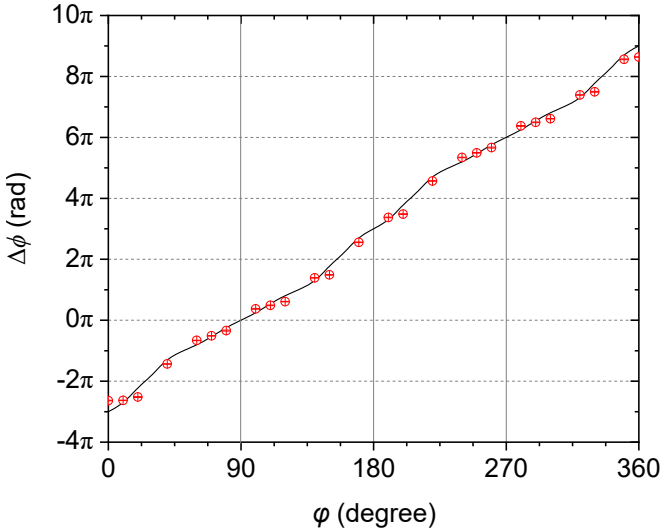


FIG. 6. Phase difference of the final state wave functions after two-photon ionization of the $2p$ initial state with $m_\ell = +1$ and -1 as a function of the photoelectron azimuthal angle.

The φ -dependence of the phase difference $\Delta\phi$ of the final-state wave functions can be derived from the data shown in Fig. 5 (right) and is presented in Fig. 6. It should be noted that extracting this phase difference is somewhat ambiguous due to the oscillatory behavior of the cosine function. In the present case we made the additional assumption that the phase increases monotonically with the azimuthal angle φ . The phase difference is $\Delta\phi = 0$ at an angle of 90° (i.e., in the y direction) due to the symmetry $\Delta\phi(90 + \varphi) = -\Delta\phi(90 - \varphi)$. Overall, the phases obtained from the experimental data are consistent and in very good agreement with the theoretical prediction, thereby supporting the validity of the two-path interference picture developed here. The remaining deviations are attributed to the blurring effects discussed in the previous paragraph. It is important to note that the method used above does not allow to unambiguously extract the individual phases of the \mathcal{A}_{2p}^+ and \mathcal{A}_{2p}^- amplitudes without using further assumptions, for example, when the angular dependence of the wave functions is expressed as a superposition of a limited set of spherical harmonics, as was done in Eq. (2).

IV. CONCLUSIONS AND OUTLOOK

We studied the details of electron emission in few-photon ionization of lithium atoms initially either in the $2s$ ground state or in the polarized $2p$ ($m_\ell = +1$) excited state by radiation close to the $2s - 2p$ resonance. We exploited the fact that the $2s$ state can be ionized through two possible pathways, specifically via the $2p$ resonance with either $m_\ell = +1$ or -1 . These two pathways interfere in the final state and resemble a double-slit. Because our experiment allows us to obtain the differential cross sec-

tions for the $2s$ and the $2p$ initial states separately, we are able to measure the final wave with both “slits” open, or with one “slit” closed. Therefore, the data make it possible to extract the interference term, thereby providing information of the phase amplitudes. The experimentally obtained phase differences are in very good agreement with our theoretical predictions.

Moreover, several interesting features are observed in the present data, which were reported for similar systems in preceding studies: First, the photoelectron angular distributions after ionization of the polarized $2p$ state are not symmetric with respect to the laser polarization. Instead, the peaks are shifted. The wavelength and intensity dependence of this effect, known as magnetic dichroism, was systematically studied in [31]. Second, the peak structures in the present angle-differential spectra are in direct contradiction to the predictions of lowest-order perturbation theory which is not applicable in resonant condition.

It is worth noting that the present method is not the only way to access information regarding the final state’s phase. The angular distributions can be fitted using model functions described by a superposition of partial waves as expressed in Eq. (2). Under certain conditions, this makes it possible to extract the relative phases between the complex amplitudes of partial waves contributing to the final state. For single-photon ionization, such *complete* studies were pioneered in the 1990s using polarized atomic targets [38–40]. In the multiphoton ionization regime, phase information was obtained by ionizing atoms with elliptically polarized light [41, 42]. In contrast, the present scheme, which exploits the resonance enhancement through two magnetic sublevels, provides direct, complete, and intuitive access to the interference term and the final-state phase.

Two- or multi-path interferences in few-photon ionization are well suited for quantum control schemes, if the relative phases and intensities of the different paths can be regulated (e.g., [26]). It is interesting to conceive such a scheme for the present system. In fact, controlling the relative (complex) amplitudes of the transient $2p$ ($m_\ell = -1$) and $2p$ ($m_\ell = +1$) populations is experimentally straightforward. The transitions from the $2s$ ground state to the two polarized excited $2p$ levels are driven by left- and right-handed circularly polarized laser radiation, respectively, propagating in the z -direction. The superposition of these two fields with equal intensity and fixed relative phase corresponds to the linearly polarized light used in the present experiment. Changing the relative phase corresponds to a rotation of the polarization direction in the xy plane.

Furthermore, a change in the relative intensities can be achieved by introducing an ellipticity to the radiation. In the present scheme, quasi-monochromatic light is used and changes of the laser polarization would also affect the ionization steps after populating the resonant $2p$ levels. However, the effect on the excitation process and the ultimate ionization could be de-coupled by using

bichromatic laser fields with a weak contribution close to the $2s - 2p$ resonance and a stronger contribution off resonance. Such an experiment would allow to prepare an atomic target in a coherent superposition of excited magnetic sublevels before ionizing it, thereby providing numerous possibilities to analyze and control the final state.

ACKNOWLEDGMENTS

The experimental material presented here is based upon work supported by the National Science Foundation under Grant No. PHY-1554776. The theoretical part of this work was funded by the NSF under grants No. PHY-2012078 (N.D.) and PHY-1803844 (K.B.), and by the XSEDE supercomputer allocation No. PHY-090031.

[1] T. Young, *Philosophical Transactions of the Royal Society of London* **92**, 12 (1802).

[2] C. J. Davisson and L. H. Germer, *Proceedings of the National Academy of Sciences* **14**, 317 (1928).

[3] C. Jönsson, *Zeitschrift für Physik* **161**, 454 (1961).

[4] D. W. Keith, C. R. Ekstrom, Q. A. Turchette, and D. E. Pritchard, *Physical Review Letters* **66**, 2693 (1991).

[5] M. Arndt, O. Nairz, J. Vos-Andreae, C. Keller, G. van der Zouw, and A. Zeilinger, *Nature* **401**, 680 (1999).

[6] L. de Broglie, *J. Physique (serie 6)* **VIII**, 225 (1927).

[7] H. Feshbach, *Annals of Physics* **5**, 357 (1958).

[8] U. Fano, *Physical Review* **124**, 1866 (1961).

[9] G. J. Schulz, *Reviews of Modern Physics* **45**, 378 (1973).

[10] C. Chin, R. Grimm, P. Julienne, and E. Tiesinga, *Reviews of Modern Physics* **82**, 1225 (2010).

[11] N. Stolterfoht, B. Sulik, V. Hoffmann, B. Skogvall, J. Y. Chesnel, J. Rangama, F. Frémont, D. Hennecart, A. Cassimi, X. Husson, A. L. Landers, J. A. Tanis, M. E. Galassi, and R. D. Rivarola, *Physical Review Letters* **87**, 023201 (2001).

[12] D. Misra, U. Kadhane, Y. P. Singh, L. C. Tribedi, P. D. Fainstein, and P. Richard, *Physical Review Letters* **92**, 153201 (2004).

[13] K. N. Egodapitiya, S. Sharma, A. Hasan, A. C. Laforgue, D. H. Madison, R. Moshammer, and M. Schulz, *Physical Review Letters* **106**, 153202 (2011).

[14] S. Zhang, D. Fischer, M. Schulz, A. Voitkiv, A. Sennfleben, A. Dorn, J. Ullrich, X. Ma, and R. Moshammer, *Physical Review Letters* **112**, 023201 (2014).

[15] D. S. Milne-Brownlie, M. Foster, J. Gao, B. Lohmann, and D. H. Madison, *Physical Review Letters* **96**, 233201 (2006).

[16] X. Li, X. Ren, K. Hossen, E. Wang, X. Chen, and A. Dorn, *Physical Review A* **97**, 022706 (2018).

[17] H. D. Cohen and U. Fano, *Physical Review* **150**, 30 (1966).

[18] M. Kunitski, N. Eicke, P. Huber, J. Köhler, S. Zeller, J. Voigtsberger, N. Schlott, K. Henrichs, H. Sann, F. Trinter, L. P. H. Schmidt, A. Kalinin, M. S. Schöffler, T. Jahnke, M. Lein, and R. Dörner, *Nature Communications* **10**, 1 (2019).

[19] H. Muller, *Applied Physics B* **74**, s17 (2002).

[20] K. Klünder, J. M. Dahlström, M. Gisselbrecht, T. Fordell, M. Swoboda, D. Guénöt, P. Johnsson, J. Caillat, J. Mauritsson, A. Maquet, R. Taïeb, and A. L'Huillier, *Physical Review Letters* **106**, 143002 (2011).

[21] M. Isinger, R. J. Squibb, D. Bustos, S. Zhong, A. Harth, D. Kroon, S. Nandi, C. L. Arnold, M. Miranda, J. M. Dahlström, E. Lindroth, R. Feifel, M. Gisselbrecht, and A. L'Huillier, *Science* **358**, 893 (2017).

[22] D. Bharti, D. Atri-Schuller, G. Menning, K. R. Hamilton, R. Moshammer, T. Pfeifer, N. Douguet, K. Bartschat, and A. Harth, *Physical Review A* **103**, 022834 (2021).

[23] Y.-Y. Yin, C. Chen, D. S. Elliott, and A. V. Smith, *Physical Review Letters* **69**, 2353 (1992).

[24] F. Ehlotzky, *Physics Reports* **345**, 175 (2001).

[25] C. Brif, R. Chakrabarti, and H. Rabitz, *New Journal of Physics* **12**, 075008 (2010).

[26] L. Giannessi, E. Allaria, K. C. Prince, C. Callegari, G. Sansone, K. Ueda, T. Morishita, C. N. Liu, A. N. Grum-Grzhimailo, E. V. Gryzlova, N. Douguet, and K. Bartschat, *Scientific Reports* **8**, 7774 (2018).

[27] P.-L. He, Z.-H. Zhang, and F. He, *Physical Review Letters* **124**, 163201 (2020).

[28] J. Pursehouse, A. J. Murray, J. Wätzel, and J. Berakdar, *Physical Review Letters* **122**, 053204 (2019).

[29] A. D. Silva, D. Atri-Schuller, S. Dubey, B. Acharya, K. Romans, K. Foster, O. Russ, K. Compton, C. Rischbieder, N. Douguet, K. Bartschat, and D. Fischer, *Physical Review Letters* **126**, 023201 (2021).

[30] A. H. N. C. D. Silva, T. Moon, K. L. Romans, B. P. Acharya, S. Dubey, K. Foster, O. Russ, C. Rischbieder, N. Douguet, K. Bartschat, and D. Fischer, *Physical Review A* **103**, 053125 (2021).

[31] B. P. Acharya, M. Dobson, S. Dubey, K. L. Romans, A. H. N. C. D. Silva, K. Foster, O. Russ, K. Bartschat, N. Douguet, and D. Fischer, *Phys. Rev. A* **104**, 053103 (2021).

[32] S. Sharma, B. P. Acharya, A. H. N. C. D. Silva, N. W. Parris, B. J. Ramsey, K. L. Romans, A. Dorn, V. L. B. de Jesus, and D. Fischer, *Physical Review A* **97**, 043427 (2018).

[33] F. Thini, K. L. Romans, B. P. Acharya, A. H. N. C. de Silva, K. Compton, K. Foster, C. Rischbieder, O. Russ, S. Sharma, S. Dubey, and D. Fischer, *Journal of Physics B: Atomic, Molecular and Optical Physics* **53**, 095201 (2020).

[34] R. Hubele, M. Schuricke, J. Gouillon, H. Lindenblatt, N. Ferreira, A. Laforgue, E. Brühl, V. L. B. de Jesus, D. Globig, A. Kelkar, D. Misra, K. Schneider, M. Schulz, M. Sell, Z. Song, X. Wang, S. Zhang, and D. Fischer, *Review of Scientific Instruments* **86**, 033105 (2015).

[35] D. Fischer, in *Ion-Atom Collisions*, edited by M. Schulz (De Gruyter, 2019) pp. 103–156.

[36] B. J. Albright, K. Bartschat, and P. R. Flicek, *Journal of Physics B: Atomic, Molecular and Optical Physics* **26**, 337 (1993).

- [37] M. Schuricke, G. Zhu, J. Steinmann, K. Simeonidis, I. Ivanov, A. Kheifets, A. N. Grum-Grzhimailo, K. Bartschat, A. Dorn, and J. Ullrich, *Physical Review A* **83**, 023413 (2011).
- [38] M. Pahler, C. Lorenz, E. v. Raven, J. Rüder, B. Sonntag, S. Baier, B. R. Müller, M. Schulze, H. Staiger, P. Zimermann, and N. M. Kabachnik, *Phys. Rev. Lett.* **68**, 2285 (1992).
- [39] U. Becker, *Journal of Electron Spectroscopy and Related Phenomena* **96**, 105 (1998).
- [40] K. Godehusen, P. Zimmermann, A. Verwegen, A. von dem Borne, P. Wernet, and B. Sonntag, *Phys. Rev. A* **58**, R3371 (1998).
- [41] F. Dulieu, C. Blondel, and C. Delsart, *Journal of Physics B: Atomic, Molecular and Optical Physics* **28**, 3845 (1995).
- [42] Z.-M. Wang and D. S. Elliott, *Physical Review Letters* **84**, 3795 (2000).